

Original citation:

Parke, L., Hooper, I. R., Hicken, R. J., Dancer, C. E. J., Grant, P. S., Youngs, I. J., Sambles, J. R. and Hibbins, A. P.. (2013) Heavily loaded ferrite-polymer composites to produce high refractive index materials at centimetre wavelengths. APL Materials, Volume 1 (Number 4). Article number 042108

Permanent WRAP url:

<http://wrap.warwick.ac.uk/57053>

Copyright and reuse:

The Warwick Research Archive Portal (WRAP) makes this work of researchers of the University of Warwick available open access under the following conditions.

This article is made available under the Creative Commons Attribution- 3.0 Unported (CC BY 3.0) license and may be reused according to the conditions of the license. For more details see <http://creativecommons.org/licenses/by/3.0/>

A note on versions:

The version presented in WRAP is the published version, or, version of record, and may be cited as it appears here.

For more information, please contact the WRAP Team at: publications@warwick.ac.uk

Heavily loaded ferrite-polymer composites to produce high refractive index materials at centimetre wavelengths

L. Parke, I. R. Hooper, R. J. Hicken, C. E. J. Dancer, P. S. Grant et al.

Citation: *APL Mater.* 1, 042108 (2013); doi: 10.1063/1.4824039

View online: <http://dx.doi.org/10.1063/1.4824039>

View Table of Contents: <http://aplmaterials.aip.org/resource/1/AMPADS/v1/i4>

Published by the [AIP Publishing LLC](#).

Additional information on APL Mater.

Journal Homepage: <http://aplmaterials.aip.org/>

Journal Information: http://aplmaterials.aip.org/about/about_the_journal

Top downloads: http://aplmaterials.aip.org/features/most_downloaded

Information for Authors: http://aplmaterials.aip.org/authors/information_for_contributors

Heavily loaded ferrite-polymer composites to produce high refractive index materials at centimetre wavelengths

L. Parke,¹ I. R. Hooper,¹ R. J. Hicken,¹ C. E. J. Dancer,^{2,3} P. S. Grant,²
 I. J. Youngs,⁴ J. R. Sambles,¹ and A. P. Hibbins¹

¹*Electromagnetic and Acoustic Materials Group, Department of Physics and Astronomy, University of Exeter, Stocker Road, Exeter EX4 4QL, United Kingdom*

²*Department of Materials, University of Oxford, Parks Road, Oxford OX1 3PH, United Kingdom*

³*WMG, University of Warwick, Coventry, CV4 7AL United Kingdom*

⁴*DSTL, Salisbury SP4 0JQ, United Kingdom*

(Received 24 July 2013; accepted 3 September 2013; published online 4 October 2013)

A cold-pressing technique has been developed for fabricating composites composed of a polytetrafluoroethylene-polymer matrix and a wide range of volume-fractions of MnZn-ferrite filler (0%–80%). The electromagnetic properties at centimetre wavelengths of all prepared composites exhibited good reproducibility, with the most heavily loaded composites possessing simultaneously high permittivity (180 ± 10) and permeability (23 ± 2). The natural logarithm of both the relative complex permittivity and permeability shows an approximately linear dependence with the volume fraction of ferrite. Thus, this simple method allows for the manufacture of bespoke materials required in the design and construction of devices based on the principles of transformation optics. © 2013 Author(s). All article content, except where otherwise noted, is licensed under a Creative Commons Attribution 3.0 Unported License. [<http://dx.doi.org/10.1063/1.4824039>]

Commercial soft ferrites, first produced by Snoek and co-workers¹ during the 1940s, have found many uses over the years due to their high permeability at low frequencies, in areas as diverse as telecommunications and antenna systems. Commercially available ferrites, such as spinel MnZn have been investigated extensively in both sintered and composite form.^{2–6} The real part of the relative permeability, (μ'_r), of sintered MnZn ferrite is high (~ 1000) up to a few MHz, but decreases rapidly above this cut off frequency, thereby restricting its useful application. On the other hand, ferrite composites in which the ferrite grains are embedded in an insulating host matrix can have a larger μ'_r at higher frequencies than the sintered material. For example, μ'_r of MnZn-ferrite composites is typically of the order of 20 up to 100 MHz,⁷ above which it decreases. This strong frequency dispersion (of both sintered and composite materials) is in accordance with Snoek's law,⁸ which states that an increase in the static permeability leads to a decrease in the cut off frequency, and vice versa. It arises from two separate phenomena: gyromagnetic spin precession and domain wall motion.

The relative real permittivity (ϵ'_r) of ferrites in their sintered and composite form vary significantly, for example, ϵ'_r of sintered NiZn ferrite can be above 2000 up to approximately 1 kHz, above which, it drops off rapidly.⁹ NiZn ferrite composites have a reduced ϵ'_r of approximately 7 (for a 50% vol. sample) up to 18 GHz, the cut off frequency, dictated by the hopping frequency of electrons within the semiconducting ferrite grains.^{10,11} Thus by moving from sintered to composite ferrimagnetic materials, it is possible to obtain non-dispersive high permittivity values over a greater frequency range.

Although there have been many investigations into ferrite-powder-polymer composites,^{12,13} it is rare that PTFE (Polytetrafluoroethylene) is chosen as the matrix material. PTFE is unusual when compared with other common polymers, such as nylon, Perspex, PPS (polyphenylene sulphide), and polypropylene, due to its ability to form a compact solid when the powdered form is compressed

at room temperature. While previous workers have used PTFE as the polymer matrix for forming MnZn ferrite composites, they have not exploited this solidifying property, and have instead heated the powder mix. For example, Yang *et al.*¹⁴ heated a 45% vol. mixture of ferrite in a PTFE matrix to 350 °C for 6 h before compressing the mixture to form a compacted solid. Cold pressed PTFE composites have been exploited by Youngs¹⁵ to produce dielectric composites; however, the % vol. of filler was only varied between 1% and 10%.

While the production of low volume fraction (below 50% vol.) ferrite composites can be trivially achieved by mixing ferrite powders with elastomers before curing,¹⁶ producing high volume fraction (above 70% vol.) composites is more challenging due to the viscosity of the mixture increasing. For example, Tsutaoka details a recipe for producing composites with volume fractions up to 75% vol. of filler using a PPS host matrix that involves mixing the two powders, melting the composite at up to 300 °C before pressing the mixture at 1000 kg/cm² while allowing it to cool over a 30 min period. In addition to this added complexity, air can become trapped in the sample, altering the density and electromagnetic properties of the composite. In order to achieve even higher % vol. samples, porous sintered ferrite composites are often used. These air–ferrite composites require temperatures of approximately 1150 °C to sinter the powder.¹⁷

In this study, a method is demonstrated for producing PTFE–ferrite composites with % vol. fractions of ferrite filler between 0% and 80%. Previous methods for producing composites across a wide range of volume fractions¹⁸ use different matrix materials and methods depending on the % vol. of filler. This is problematic as direct comparisons between samples manufactured using different techniques cannot be made. Our method provides a simple and reliable method for fabrication of electromagnetic materials with user-specified μ'_r and ϵ'_r values, important in the field of metamaterials. The technique can be extended to many different filler materials and more complex, for example three part, composites and avoids the need to use elevated temperatures.

The ferrite chosen for this study was a commercially available sintered MnZn ferrite powder (grade F44) supplied by MagDev Ltd (UK). Using x-ray diffraction, the phase composition was found to be $\text{Zn}_{0.2}\text{Mn}_{0.8}\text{Fe}_2\text{O}_4$ with some minor impurity phases (Fe_3O_4 , Fe_2O_3 , MnO). The static μ'_r and ϵ'_r as specified by the manufacturer were 1.5×10^3 and 1.0×10^5 , respectively. The median ferrite particle diameter determined by laser diffraction with the powder dispersed in deionised water using an ultrasonic probe (Mastersizer2000, Malvern Instruments Ltd, UK) was 35 μm , while the range of particle sizes spanned from $<1 \mu\text{m}$ to 500 μm , with the mass mean particle diameter of the PTFE powder determined by the manufacturer (Sigma Aldrich Ltd.) to be 35 μm .

MnZn ferrite (filler) and PTFE (matrix) powders were mixed together with filler volume ratios ranging from 10% to 80%, and pressed in a steel mould under 55 MPa for 300 s. Five pairs of samples were made for each ferrite fraction to verify reproducibility.

A stripline technique developed by Barry in 1986¹⁹ was used to characterise the ferrite-composite samples, with one half of each sample-pair positioned above the signal line, and the other half below. The stripline is connected to a calibrated vector network analyser (VNA) that quantifies the complex reflection and transmission amplitude coefficients of samples. From the complex reflection and transmission amplitude coefficients together with the frequency and the thickness of the sample, the relative complex permittivity (ϵ_r) and permeability (μ_r) can be obtained using the Nicholson, Ross, Weir (NRW) extraction method.^{20,21} One sample from each pair has a channel milled down its centre to fit the stripline. This eliminates air gaps between opposite sample faces on either side of the central signal line. The top and bottom faces of each sample are metalized over the area intended to be in contact with the stripline by depositing by vacuum evaporation 60 nm of silver (see Figure 1). This provides a continuous conducting plane at the boundary of the composite sample, and ensures that any remaining small air gaps between the high permittivity samples and the stripline electrodes, arising from surface roughness or errors associated with the milling process, are shorted out. The capacitance associated with such gaps, even if of order 10 μm in an otherwise filled system would alter the results significantly for high ϵ'_r samples, and lead to erroneous extracted ϵ'_r values.

Backscattered scanning electron microscopy (840A SEM, JEOL – tungsten filament at 20 kV) images (Figure 2) of ferrite composites for (a) and (b) 10% vol. filler and (c) and (d) 70% vol. filler were examined to visualise ferrite particle distribution in the PTFE matrix. Samples were cut using

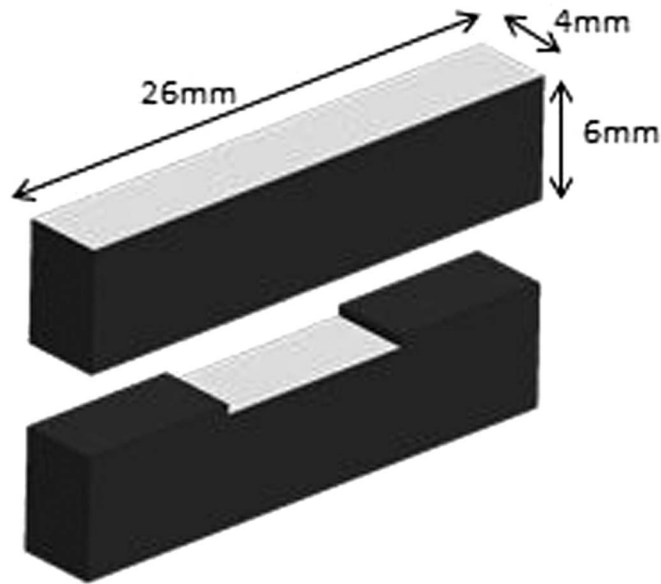


FIG. 1. Illustration of both halves of the ferrite composite sample pair machined to fit above and below the signal line, for stripline characterisation. Top and bottom surfaces of both parts are metalized with 60 nm of silver over the areas intended to be in contact with the stripline.

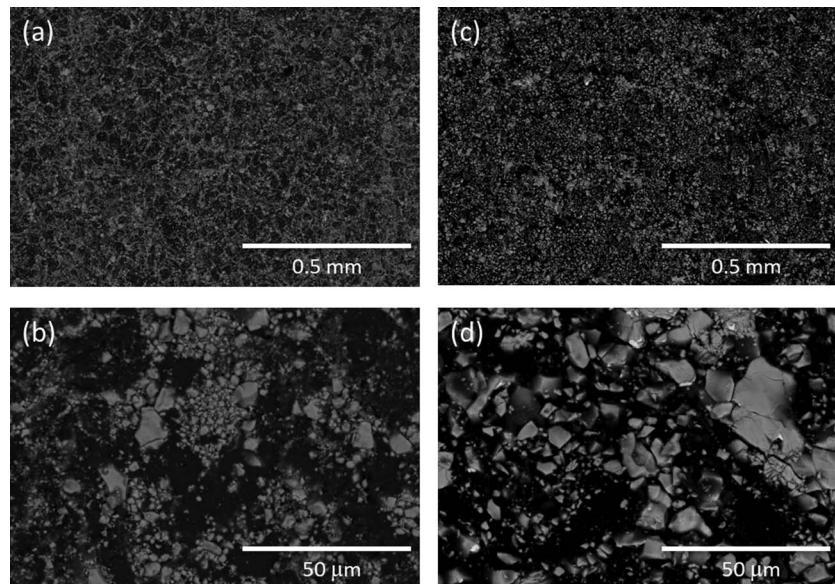


FIG. 2. Backscattered scanning electron microscopy images showing cross-sections through MnZn ferrite composites of different volume fractions. (a) and (b) 10% vol. sample; (c) and (d) 70% vol. sample.

a diamond saw (Isomet 1000, Buehler), mounted using silver paint, and coated with a thin layer of carbon to prevent charging in the SEM. The images show ferrite particles as light regions in the darker PTFE matrix. Although there is evidence of agglomeration of ferrite particles, as well as a slightly uneven distribution, the PTFE has spread throughout the ferrite sufficiently such that there were no large clusters of MnZn ferrite particles.

The mass densities, ρ , of the samples were established by determining the volume (using vernier calipers, capable of measuring to within 0.01 mm, the width, thickness, and length of samples were measured at 3 different positions along each axis and averaged.) and weight (using

TABLE I. Predicted and experimental data (averaged over five pairs of samples for each concentration with the standard deviation) for densities ρ of ferrite-PTFE composites.

% vol.	ρ predicted (g/cm ³)	Average ρ experiment (g/cm ³)
10	2.46	2.45 ± 0.02
30	2.90	2.87 ± 0.04
50	3.50	3.50 ± 0.02
70	4.02	4.01 ± 0.06
80	4.28	4.24 ± 0.11

an electronic balance sensitive to within 0.1 g). These experimental values were compared with calculated densities to verify whether cold pressing had eliminated all air gaps (Table I). To within the accuracy of measurement, all samples had the expected density, demonstrating that this cold pressing method produces fully dense samples across the full range of ferrite fractions.

Results for the average ϵ_r and μ_r of each set of five samples at 50 MHz for the different % vol. concentrations are listed in Table II.

It is well known that applying high pressures to soft ferrimagnetic materials such as MnZn ferrite can alter their magnetic response²² by introducing additional anisotropy, causing a shift in the gyromagnetic frequency. Since the fabrication process involves high pressure compression of a powder mix followed by subsequent milling some variations between samples are likely to be exhibited, particularly in μ'_r results.

The average ϵ'_r as a function of frequency for five pairs of samples at each volume concentration is shown in Figure 3(a). For all samples, ϵ'_r remains approximately constant up to a cut-off frequency. Although ϵ'_r increases with increased % vol. of filler, the cut-off frequency for all the composites is also approximately the same. This is due to the ferrite powder consisting of semi-conducting grains encapsulated by dielectric layers. At low frequencies, electron hopping occurs between Fe^{3+} and Fe^{2+} on the octahedral sites.²³ The electrons reach the phase boundaries between the ferrite and PTFE through hopping and thus accumulate at these phase boundaries, which results in interfacial polarization. As the frequency is increased, the hopping frequency increases until the electrons can no longer follow the applied electric field causing ϵ'_r to drop.⁹ The frequency dispersion of μ'_r is displayed in Fig. 3(b), it is approximately constant from 10 MHz to 100 MHz for high vol.% samples, and from 10 MHz to 1 GHz for low vol.% samples before dropping rapidly as the gyromagnetic resonance frequency is approached. The simultaneously high ϵ'_r and μ'_r values at low frequencies make this material an excellent candidate to produce ultra-high refractive index and impedance matched materials required in the field of transformation optics.

The Lichtenecker mixing formula is a widely used empirical and analytical model for predicting the filler fraction dependence of ϵ'_r (Eq. (1)) and μ'_r (Eq. (2)) of well dispersed composite materials,^{24,25}

$$\ln(\epsilon_{\text{composite}}) = f \ln(\epsilon_{\text{MnZn}}) + (1 - f)\ln(\epsilon_{\text{PTFE}}), \quad (1)$$

$$\ln(\mu_{\text{composite}}) = f \ln(\mu_{\text{MnZn}}) + (1 - f)\ln(\mu_{\text{PTFE}}). \quad (2)$$

Here f is the volume fraction of ferrite, $\epsilon_{\text{composite}}$ and $\mu_{\text{composite}}$ are the relative permittivity and permeability of the composite, ϵ_{MnZn} and μ_{MnZn} are the relative permittivity and permeability of the bulk MnZn ferrite, and ϵ_{PTFE} and μ_{PTFE} are the relative permittivity and permeability of bulk PTFE.

Figure 4 illustrates the validity of the Lichtenecker mixing formula for our data by demonstrating the linear relationship between the natural logarithms containing ϵ'_r (a), ϵ''_r (b), and μ'_r and μ''_r (c), against % vol. of the ferrite filler. From Figure 4 it is possible to predict ϵ_r and μ_r for this ferrite composite at all % vol. Note that this logarithmic mixing law has been

TABLE II. Average real and imaginary parts of the relative permittivity and permeability of the composite with standard deviation at 50 MHz determined from the stripline measurements of the sets of 5 samples for each% vol.

	10% vol.	30% vol.	50% vol.	70% vol.	80% vol.
ϵ'_r	5.2 ± 0.2	13 ± 1	46 ± 3	96 ± 4	177 ± 10
μ'_r	1.22 ± 0.20	2.90 ± 0.03	9 ± 1	16 ± 1	21 ± 1
ϵ''_r	0.02 ± 0.04	0.25 ± 0.17	0.63 ± 0.25	2.7 ± 1.7	5.2 ± 2.5
μ''_r	0.97 ± 0.04	0.17 ± 0.04	2.7 ± 0.1	2.8 ± 0.1	4.5 ± 0.3

shown previously for a range of materials including carbon fibre, γ -Fe₂O₃, and carbonyl iron composites.^{26–28}

To fit to our measurements of ϵ'_r in Figure 4(a), we utilize the relationship stated in Eq. (3). Here we assume the relative imaginary permittivity of the PTFE is zero and that it may be neglected for the ferrite as the real part is significantly higher than the corresponding imaginary part

$$\ln \epsilon'_{\text{composite}} = f \ln \frac{\epsilon'_{\text{MnZn}}}{\epsilon'_{\text{PTFE}}}, \quad (3)$$

where ϵ'_{MnZn} is the real part of the relative permittivity of the pure ferrite, ϵ'_{PTFE} is the real part of the relative permittivity of the pure PTFE, f is the volume fraction of the ferrite, and $\epsilon'_{\text{composite}}$ is the real part of the relative permittivity of the composite at a given volume fraction of ferrite. The relationship was obtained as a result of a first order approximation assuming $\epsilon''_{\text{MnZn}} \ll \epsilon'_{\text{MnZn}}$ in the Lichtenecker formula. A first order approximation is possible in this case as MnZn ferrite composites have a dielectric loss tangent of ~ 0.03 (at 80% vol.) or smaller, classifying them as low dielectric loss materials. In order to obtain ϵ''_r , the following relationship is used:

$$\frac{\epsilon''_{\text{composite}}}{\epsilon'_{\text{composite}}} = f \frac{\epsilon''_{\text{MnZn}}}{\epsilon'_{\text{MnZn}}}, \quad (4)$$

where ϵ'_{MnZn} is the ϵ'_r of the pure ferrite, and $\epsilon''_{\text{composite}}$ is the ϵ''_r of the composite at a given volume fraction of ferrite. This relationship was obtained by substituting ϵ_r into the Lichtenecker mixing formula, and assuming $\epsilon_{\text{im PTFE}} = 0$.

The real and imaginary parts of μ_r cannot be separated in the same way as for ϵ_r as the imaginary part is not much smaller than the real part. From the Lichtenecker formula, the natural log of the sum of squares for μ'_r and μ''_r versus the volume fraction gives a linear relationship. This has been presented graphically in Fig. 4(c) and analytically using the following relationship (assuming μ'_r of PTFE is 1):

$$\ln(\mu'_{\text{composite}}{}^2 + \mu''_{\text{composite}}{}^2) = f \ln(\mu'_{\text{MnZn}}{}^2 + \mu''_{\text{MnZn}}{}^2), \quad (5)$$

where $\mu'_{\text{composite}}$ is the relative real permeability of the composite, $\mu''_{\text{composite}}$ is the relative imaginary permeability of the composite, μ'_{MnZn} is the relative real permeability of bulk ferrite, and μ''_{MnZn} is the relative imaginary permeability of bulk ferrite.

To extract the value of μ_r at 100% vol. of filler, two relations containing both μ'_r and μ''_r terms are solved simultaneously. From the straight line fit from Fig. 4(c) we find

$$\ln(\mu'_{\text{MnZn}}{}^2 + \mu''_{\text{MnZn}}{}^2) = 8 \pm 0.5. \quad (6)$$

Also the average magnetic loss tangent for all 5 data sets (10%, 30%, 50%, 70%, and 80% vol.) is

$$\frac{\mu''_{\text{composite}}}{\mu'_{\text{composite}}} = 1.8 \pm 0.04. \quad (7)$$

This simple extraction of effective μ_r and ϵ_r for 100% vol. of ferrite allows the estimation of the electromagnetic properties of ferrite composites with any% vol.

In summary, a cold pressing method for producing ferrite-PTFE composites for filler fractions from 0% to 80% has been reported. The simplicity and reproducibility of this method across the

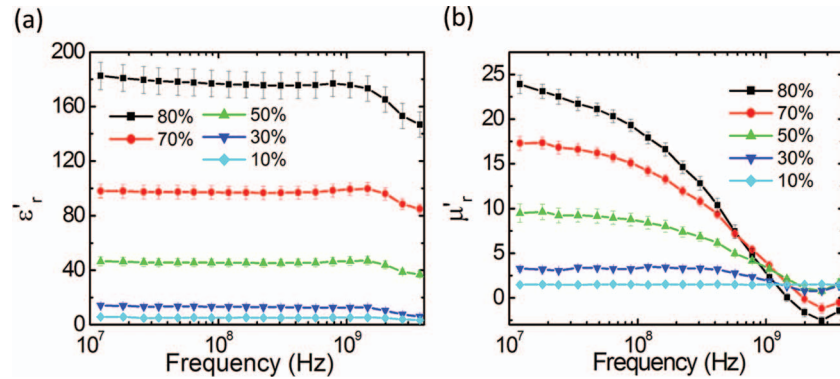


FIG. 3. Frequency dispersion of (a) ϵ'_r and (b) μ'_r for different % vol. of filler. Results for each % vol. are the average with the standard deviation from separate data sets for 5 independently made composites.

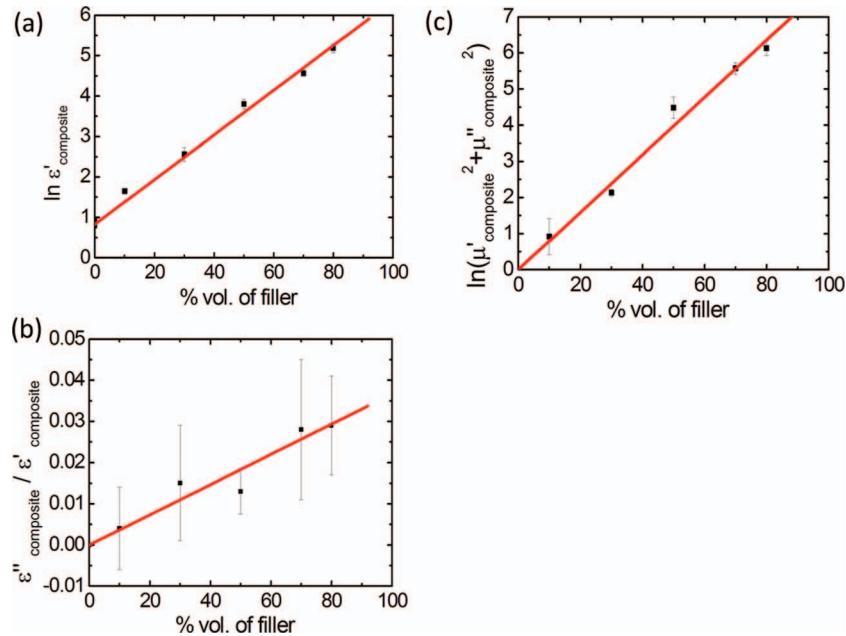


FIG. 4. (a) Natural log of the average relative real permittivity $\epsilon'_{\text{composite}}$ of the composite (b) average dielectric loss tangent of the composite $\epsilon''_{\text{composite}}/\epsilon'_{\text{composite}}$ and (c) natural log of the modulus of the average relative permeability squared plus the average relative imaginary permeability squared for the composite $\ln(\mu'^2_{\text{composite}} + \mu''^2_{\text{composite}})$ as a function of % vol. at 50 MHz for MnZn ferrite-PTFE composites.

full range of filler fractions has been demonstrated by comparing the electromagnetic response of independently manufactured samples. The simultaneously high static permittivity (180 ± 10) and permeability (23 ± 2) of 80% vol. composites can be used to create high refractive index and impedance matched devices important in the field of transformation optics. Data for both permittivity and permeability accord well with the simple Lichtenecker formula, enabling it to be used to predict desired material properties. The cold pressing method used the same matrix material and sample manufacture technique across the full range of volume fractions and can be extended for use with a variety of different filler materials.

ACKNOWLEDGMENTS

The authors wish to acknowledge the financial support of the EPSRC and DSTL for funding LP's Ph.D. studentship through the University of Exeter Doctoral Training account, MagDev,

and J.R.S., I.R.H., C.E.J.D., I.J.Y., P.S.G., and A.P.H. through the QUEST programme Grant No. (EP/I034548/1) “The Quest for Ultimate Electromagnetics using Spatial Transformations.”

- ¹ A. Goldman, *Modern Ferrite Technology*, 2nd ed. (Springer, Van Nostrand Reinhold, 2010), Chap. 8, p. 217.
- ² H. I. Hsiang, W. S. Chen, Y. L. Chang, F. C. Hsu, and F. S. Yen, *Am. J. Mater. Sci.* **1**, 40 (2011).
- ³ E. F. Schlömann, *J. Appl. Phys.* **41**, 204 (1970).
- ⁴ A. Globus, *J. Phys. Colloq.* **38**, C1 (1977).
- ⁵ J. P. Bouchaud and P. G. Zerah, *J. Appl. Phys.* **67**, 5512 (1990).
- ⁶ *Ferromagnetic Materials*, edited by E. P. Wohlfarth (North-Holland, Amsterdam, 1980), p. 243.
- ⁷ R. Dousoudil, M. Usakove, J. Franek, J. Slama, and A. Gruskova, *IEEE Trans. Magn.* **46**, 436 (2010).
- ⁸ J. L. Snoek, *Physica* **14**, 207 (1948).
- ⁹ C. G. Koops, *Phys. Rev.* **83**, 121 (1951).
- ¹⁰ L. B. Kong, Z. W. Li, G. Q. Lin, and Y. B. Gan, *IEEE Trans. Magn.* **43**, 6 (2007).
- ¹¹ D. L. Zhao, Q. Li, and Z. M. Shen, *J. Alloys Compd.* **480**, 634 (2009).
- ¹² L. Valko, P. Bucek, R. Dosoudil, and M. Ušáková, *J. Electr. Eng.* **54**, 100 (2003).
- ¹³ J. Rekošová, R. Dosoudil, M. Ušáková, E. Ušák, and I. Hudec, *IEEE Trans. Magn.* **49**, 38 (2013).
- ¹⁴ H. B. Yang, Y. Lin, and F. Wang, *Key Eng. Mater.* **368–372**, 629 (2008).
- ¹⁵ I. J. Youngs, *J. Phys. D: Appl. Phys.* **36**, 738 (2003).
- ¹⁶ J. Kruželák, R. Dosoudil, I. Hudec, and R. Sykora, *J. Electr. Eng.* **63**, 137 (2012).
- ¹⁷ T. Takanori, *J. Appl. Phys.* **93**, 2789 (2003).
- ¹⁸ R. Moucka, A. Lopatin, N. Kazantseva, J. Vilcakova, and P. Saha, *J. Mater. Sci.* **42**, 9480 (2007).
- ¹⁹ W. Barry, *IEEE Trans. Microwave Theory Tech.* **34**, 80 (1986).
- ²⁰ A. M. Nicolson and G. F. Ross, *IEEE Trans. Instrum. Meas.* **19**, 377 (1970).
- ²¹ W. W. Weir, *Proc. IEEE* **62**, 33 (1974).
- ²² M. LeFlo'c'h, J. Loaec, H. Pascard, and A. Globus, *IEEE Trans. Magn.* **17**, 1218 (1981).
- ²³ M. J. Iqbal, Z. Ahmad, T. Meydan, and Y. Melikhov, *J. Appl. Phys.* **111**, 033906 (2012).
- ²⁴ K. Lichtenecker and K. Rother, *Z. Phys.* **32**, 255 (1931).
- ²⁵ R. Simpkin, *IEEE Trans. Microwave Theory Tech.* **58**, 545 (2010).
- ²⁶ C. P. Neo and V. K. Varadan, *IEEE Trans. Electromagn. Compat.* **46**, 102 (2004).
- ²⁷ J. B. Birks, *Proc. Phys. Soc.* **60**, 282 (1948).
- ²⁸ K. C. Pitman, M. W. Lindley, D. Simkin, and J. F. Cooper, *IEE Proceedings F* **138**, 223 (1991).